Yemen Journal of Medicine

https://yemenjmed.com

Article information

DOI: 10.63475/yjm.v4i3.0244

Article history:
Received: 07 December 2025
Accepted: 22 December 2025
Published: 31 December 2025

Correspondence to:
Tajudeen Afolayan Lawal
Email: lawalat40@gmail.com
ORCID: 0000-0002-9623-6266

How to cite this article
Lawal TA, Sholadoye QO. Antioxidant and antidiabetic enzyme inhibitory activity of the ethyl acetate fraction of Ocimum gratissimum leaf methanol extract. Yemen J Med.2025;4(3): 613-623.

Original Article

Antioxidant and Antidiabetic Enzyme Inhibitory Activities of the Ethyl Acetate Fraction of *Ocimum gratissimum* Leaf Methanol Extract

Tajudeen Afolayan Lawal[1], Qazeem Oyeniyi Sholadoye[2]

1 Lecturer, Biochemistry and Forensic Science Department, Faculty of Science, Nigeria Police Academy, Wudil, Kano, Nigeria
2 Lecturer, Chemistry Department, Faculty of Science, Nigeria Police Academy, Wudil, Kano, Nigeria

ABSTRACT

Background: Natural products remain an important source of bioactive compounds for the management of metabolic disorders. This study aimed to investigate the antidiabetic and antioxidant potential of the ethyl acetate fraction of *Ocimum gratissimum* leaves (EAFOGL) through in vitro enzyme inhibition assays, antioxidant assays, and molecular docking analyses, to identify the phytochemicals responsible for the observed bioactivities.

Methods: EAFOGL was evaluated for α-amylase and α-glucosidase inhibitory activities and antioxidant potential using radical scavenging and metal chelation assays. Molecular docking was performed for selected phytochemicals against α-amylase (PDB ID: 1B2Y), α-glucosidase (PDB ID: 2QMJ), and xanthine oxidase (PDB ID: 3NVY). Docking protocol validation was achieved by re-docking native ligands, and binding affinities and protein–ligand interactions were analysed.

Results: EAFOGL exhibited moderate inhibition of α-amylase (IC_{50} = 87.17 ± 5.20 µg/mL) and α-glucosidase (IC_{50} = 49.84 ± 6.72 µg/mL) compared with acarbose (IC_{50} = 52.12 ± 2.74 and 40.94 ± 3.44 µg/mL, respectively). The fraction also demonstrated notable radical scavenging (IC_{50} = 90.32 ± 9.91 µg/mL) and metal chelating (IC_{50} = 98.58 ± 13.29 µg/mL) activities, although less potent than ascorbic acid and Ethylenediaminetetraacetic acid (EDTA). Docking validation yielded root mean square deviation values below 2.0 Å, confirming docking reliability. Among the screened compounds, rosmarinic acid isomers showed favourable binding energies and strong interactions with key catalytic residues of all three enzymes. Notably, cis-rosmarinic acid exhibited the highest affinity toward xanthine oxidase (−7.558 kcal/mol), exceeding that of the native ligand quercetin.

Conclusions: The findings demonstrate that EAFOGL possesses moderate antidiabetic and antioxidant activities, supported by molecular docking results identifying rosmarinic acid derivatives as key contributors to enzyme inhibition. These results highlight EAFOGL as a promising source of bioactive compounds for managing oxidative stress and postprandial hyperglycaemia.

Key words: *Ocimum gratissimum*, α-amylase inhibition, α-glucosidase inhibition, antioxidant activity, molecular docking, rosmarinic acid, xanthine oxidase

INTRODUCTION

The global prevalence of type 2 diabetes mellitus (T2DM) is rising at an alarming rate, posing a major public health challenge worldwide. [1] T2DM is characterised by chronic hyperglycaemia and insulin resistance and is associated with severe complications, including cardiovascular disease, nephropathy, and neuropathy. [2] A key therapeutic strategy for managing postprandial hyperglycaemia involves the inhibition of digestive enzymes such as α-amylase and α-glucosidase, which catalyse the hydrolysis of complex

carbohydrates into absorbable glucose units. [1,2] Beyond chronic hyperglycaemia, oxidative stress plays a pivotal role in the development of T2DM. [3] The overproduction of reactive oxygen species (ROS) interferes with insulin signalling pathways and induces damage to pancreatic β-cells, thereby contributing to insulin resistance and dysregulated glucose metabolism. [4] Consequently, there is growing interest in therapeutic compounds that combine antioxidant activity with enzyme-inhibitory effects, such as α-amylase and α-glucosidase inhibition, to simultaneously mitigate oxidative damage and control postprandial hyperglycaemia. [5]

Ocimum gratissimum L. (African basil) is a widely used medicinal plant in tropical Africa and Asia, traditionally employed in the management of type 2 diabetes, inflammatory conditions, and microbial infections. [6] Although the therapeutic potential of its crude extracts has been well documented, evidence on the biological activities of its semi-purified ethyl acetate fraction remains limited, particularly with respect to antidiabetic and antioxidant mechanisms. [7] Experimental studies have demonstrated that *O. gratissimum* leaf extracts exert significant hypoglycaemic and antioxidant effects in diabetic rodent models. Methanolic crude extracts and solvent-partitioned fractions, including the ethyl acetate fraction (EAFOGL), have been shown to improve fasting blood glucose, insulin levels, and insulin sensitivity in streptozotocin-induced type 2 diabetic rats; however, the n-butanol fraction frequently exhibited superior efficacy in attenuating hyperglycaemia and associated biochemical abnormalities. [8] Similarly, aqueous leaf extracts have been reported to enhance endogenous antioxidant defence systems in vivo, evidenced by increased activities of superoxide dismutase and catalase and reduced lipid peroxidation, highlighting a role in oxidative stress modulation. [9]

Inhibiting α-amylase and α-glucosidase enzymes slows carbohydrate digestion and glucose absorption, thereby reducing postprandial blood glucose spikes. [10] Although acarbose, a standard synthetic inhibitor, has demonstrated clinical efficacy in glycaemic control, its long-term use is limited due to gastrointestinal side effects such as flatulence and diarrhoea. Consequently, there is growing interest in plant-derived enzyme inhibitors, which are believed to offer similar therapeutic benefits with fewer adverse effects. [11]

Oxidative stress, defined as an imbalance between the generation of ROS and antioxidant defences, is implicated in the pathogenesis of metabolic, cardiovascular, and inflammatory disorders through ROS-induced damage to lipids, proteins, and DNA. [12] Oxidative stress exacerbates hyperglycaemia and accelerates diabetic complications by promoting molecular damage and cellular dysfunction. Antioxidants scavenge free radicals, improve insulin sensitivity, and protect pancreatic β-cells. Accordingly, antioxidant assays such as 2,2-diphenyl-1-picrylhydrazyl (DPPH) radical scavenging and metal ion chelation provide essential screening tools for identifying natural compounds with redox-modulating potential. [13]

Elevated xanthine oxidase (XO) activity significantly contributes to ROS production during purine catabolism by generating superoxide anions and hydrogen peroxide, thereby exacerbating oxidative stress and associated tissue injury in conditions such as diabetes and its complications. [12] Inhibition of XO has been shown to attenuate oxidative damage and improve metabolic and vascular dysfunction in disease models, underscoring its pathological role and therapeutic relevance. XO-derived ROS have been linked to enhanced oxidative stress in diabetic skeletal muscle and vascular tissues, and XO inhibition has been reported to ameliorate oxidative injury and downstream signalling disturbances in diabetic kidney disease. [14] Collectively, these findings highlight XO as a key enzymatic source of ROS in oxidative stress–related pathologies and a relevant target in the search for natural antioxidants and enzyme inhibitors.

This research aimed to assess the inhibitory effects of the ethyl acetate fraction of *O. gratissimum* extract (EAFOGL) on α-amylase and α-glucosidase enzymes, along with its antioxidant potential using DPPH and metal chelation assays. Additionally, it aims to identify the phytochemical constituents through Liquid Chromatography-Mass Spectrometry (LC-MS) analysis and explore the molecular docking interactions of key bioactive compounds. The overarching objective is to offer scientific evidence supporting its potential use in the treatment of diabetes and oxidative stress-related conditions.

MATERIALS AND METHODS

Plant Collection, Extraction, and Fractionation

Fresh, healthy leaves of *Ocimum gratissimum* L. were collected from a mature plant located in the herbarium section of the Department of Plant Science and Biotechnology, Bayero University, Kano, Nigeria, on April 22, 2025. The plant material was identified by botanist Mallam Ibrahim Shu'aibu and authenticated by Prof. Hajara Haruna, and a voucher specimen was deposited with herbarium number BUKHAN00306. The research was carried out between May 3, 2025, and October 30, 2025.

Extraction and Fractionation

The leaves were air-dried, ground into a fine powder, and extracted with 80% methanol (1:10 w/v) by cold maceration for 72 hours with intermittent shaking. The extract was filtered and concentrated under reduced pressure at 40 °C using a rotary evaporator to obtain the crude methanol extract. Sequential solvent partitioning was performed using n-hexane, chloroform, ethyl acetate, and n-butanol. The ethyl acetate fraction (EAFOGL) was selected for further phytochemical, antioxidant, enzyme inhibition, and *in silico* analyses based on preliminary bioactivity screening and its enrichment of phenolic and flavonoid compounds.

Enzyme Inhibition Assays

α*Amylase inhibition (DNSA method)*

The α-amylase inhibitory activity of the ethyl acetate fraction of *O. gratissimum* leaves (EAFOGL) was evaluated using the dinitrosalicylic acid (DNSA) colorimetric assay, following a method adapted from Dev-Sharma et al. [15] Briefly, 250 µL of EAFOGL at varying concentrations (25–150 µg/mL) was pre-incubated with 125 µL of α-amylase solution (5 mg/mL) prepared in 0.02 M sodium phosphate buffer (pH 6.9) at 25°C for 10 minutes. Subsequently, 500 µL of 2% (w/v) soluble starch solution was added as the substrate, and the mixture was further incubated at 25°C for 10 minutes. The enzymatic reaction was terminated by the addition of 500 µL

of DNSA reagent, followed by heating in a boiling water bath (100°C) for 10 minutes to develop the colour. After cooling to room temperature, the absorbance was measured spectrophotometrically at 540 nm.

A negative control (blank) was prepared by replacing the extract with the phosphate buffer, representing 100% enzyme activity, while a positive control containing acarbose at equivalent concentrations was assayed under identical conditions to validate the inhibitory response. All assays were performed in triplicate. The percentage α-amylase inhibition was calculated using the standard formula shown in **Equation 1**.

$$\% \text{ Enzyme inhibition} = \frac{A_0 - A_f}{A_0} \times 100 \quad (1)$$

Where A_0 is the absorbance of the blank (negative control) without the fraction, while A_f is the absorbance with the fraction or acarbose. The IC_{50} values were determined by fitting the inhibition data to a nonlinear regression model using a sigmoidal dose–response (variable slope) equation, as described by Motulsky and Christopoulos. [16]

α-Glucosidase Inhibition (pNPG Method)

The α-glucosidase inhibitory activity of the EAFOGL was evaluated using p-nitrophenyl-α-D-glucopyranoside (pNPG) as the substrate, following the method described by Lawal et al. [17] Briefly, 50 µL of EAFOGL at varying concentrations (25–150 µg/mL) was pre-incubated with 100 µL of α-glucosidase solution prepared in phosphate buffer (pH 6.9) at 37°C for 10 minutes. Subsequently, 50 µL of 5 mM pNPG was added to initiate the reaction. After incubation at 37°C for 5 minutes, the reaction was terminated by the addition of 2 mL of 0.5 M sodium carbonate, and the release of p-nitrophenol was quantified by measuring the absorbance at 405 nm.

A negative control, containing enzyme and substrate without the extract, was used to represent 100% α-glucosidase activity, while acarbose, assayed under identical conditions and at corresponding concentrations, served as the positive control. All experiments were conducted in triplicate, and the percentage inhibition of α-glucosidase activity was calculated using the standard equation shown in Equation 1. The IC_{50} values were determined accordingly.

Antioxidant Assays

DPPH Radical Scavenging Assay

The free radical scavenging capacity of EAFOGL was evaluated using the DPPH assay, as described by Gulcin and Alwasel. [18] Briefly, 1 mL of freshly prepared 0.1 mM DPPH solution in methanol was mixed with 1 mL of EAFOGL at varying concentrations (25, 50, 75, 100, 125, and 150 µg/mL). The reaction mixture was incubated in the dark at room temperature for 30 minutes, after which the decrease in absorbance was measured spectrophotometrically at 517 nm. Ascorbic acid served as the reference antioxidant standard. The percentage radical scavenging activity (RSA) of EAFOGL was calculated using the equation presented in **Equation 2**.

$$\text{RSA (\%)} = \frac{A_C - A_S}{A_C} \times 100 \quad (2)$$

where A_C is the absorbance of the negative control sample (i.e., without the EAFOGL), and A_S is the absorbance that contains EAFOGL, or ascorbic acid. The IC_{50} was calculated from the graph plotting scavenging percentage against test sample concentration (µg/mL).

Metal Chelating Activity

The ferrous ion–chelating activity of EAFOGL was evaluated using the method of Gulcin and Alwasel. [19] Briefly, varying concentrations (25–150 µg/mL) of the EAFOGL and EDTA (standard) were mixed with 0.05 mL of 2 mM $FeCl_2$ solution to initiate chelation of Fe^{2+} ions by the samples. The reaction was prompted by the addition of 0.2 mL of 5 mM ferrozine reagent, followed by gentle mixing. The mixture was then incubated at 25°C for 10 minutes. After incubation, the absorbance was measured at 562 nm to assess the formation of the Fe^{2+}–ferrozine complex. The percentage inhibition of complex formation was calculated relative to the control. The percentage chelating ability of EAFOGL and EDTA is determined using **Equation 3**:

$$\% \text{ Chelating effect} = \frac{A_0 - A_1}{A_0} \times 100 \quad (3)$$

Where A_0 and A_1 are the absorbances of the control (without EAFOGL or EDTA) and sample (with EAFOGL or EDTA), respectively. The IC_{50} was calculated from the graph plotting percentage chelating effect against EAFOGL and EDTA concentration (µg/mL).

LC-MS Analysis

For LC-MS analysis, a known quantity of the ethyl acetate fraction of *O. gratissimum* leaves (EAFOGL) was dissolved in HPLC-grade methanol to obtain a final concentration of approximately 1 mg/mL and filtered through a 0.22 µm PTFE membrane filter to remove particulate matter. An aliquot (5–10 µL) of the prepared sample was injected into an LC-MS system equipped with a reversed-phase C18 analytical column (e.g., 150 × 2.1 mm; 1.7–3.5 µm particle size), maintained at 30 to 40°C. Chromatographic separation was achieved using a gradient elution program consisting of solvent A (water containing 0.1% formic acid) and solvent B (acetonitrile containing 0.1% formic acid), at a flow rate of 0.2 to 0.4 mL/min. A typical gradient profile was as follows: 5% B (0–2 minutes), 5% to 95% B (2–25 minutes), held at 95% B (25–30 minutes), followed by re-equilibration to initial conditions. The total run time was approximately 35 minutes.

Eluted analytes were introduced into an electrospray ionisation (ESI) source operated in both positive and negative ionisation modes under optimised conditions, including capillary voltage of 3.0 to 4.5 kV, desolvation temperature of 300 to 350°C, nebulising gas flow of 600 to 800 L/h, and cone voltage of 20 to 40 V. Mass spectra were acquired over an m/z range of 100 to 1500 using high-resolution mass spectrometers such as Q-TOF or Orbitrap systems, ensuring mass accuracy within ±5 ppm. Data-dependent MS/MS experiments were performed using collision-induced dissociation or higher-energy collisional dissociation with collision energies ranging from 10 to 40 eV to generate characteristic fragmentation patterns. Tentative identification of detected compounds was achieved by comparing accurate mass measurements,

retention times, and MS/MS fragmentation spectra with reference standards and online spectral databases, including METLIN and MassBank (https://massbank.eu/MassBank). Only compounds with acceptable mass errors, isotopic pattern matching, and diagnostic fragment ions were reported. This analytical procedure was conducted in accordance with established methodologies described by Pang et al., [20] Abilkassymova et al., [21] and Breaud et al. [22]

It should be noted that compound identification in this study was tentative, as it was primarily based on accurate mass measurements, chromatographic retention behaviour, and MS/MS fragmentation pattern matching with spectral libraries (METLIN and MassBank). In the absence of authentic reference standards for all detected compounds, definitive structural confirmation could not be achieved. Consequently, isomeric compounds with identical molecular formulas and similar fragmentation patterns may not have been fully resolved. However, the use of high-resolution mass spectrometry with strict mass error thresholds (≤5 ppm), diagnostic fragment ions, and database cross-validation provides a reliable level of confidence for phytochemical annotation. Further confirmation using purified standards and complementary spectroscopic techniques, such as Nuclear Magnetic Resonance (NMR), is recommended in future studies.

Molecular Docking Studies

In silico molecular docking analysis was performed following the protocol described by Lawal et al. [23] to evaluate the binding affinities and interaction profiles of selected phytochemicals identified from the extract against key diabetes- and oxidative stress-related protein targets, namely α-amylase (PDB ID: 1B2Y), α-glucosidase (PDB ID: 2QMJ), and XO (PDB ID: 3NVY). The crystallographic three-dimensional structures of the target proteins were retrieved from the Protein Data Bank (https://www.rcsb.org) and prepared using the Molecular Operating Environment (MOE) software (version 2015.10). Protein preparation involved the removal of co-crystallised ligands, water molecules beyond 5 Å from the active site, and other heteroatoms, followed by the addition of missing hydrogen atoms. Protonation states were assigned at physiological pH (7.4), and energy minimisation was carried out using the AMBER10:EHT force field until a root mean square gradient of 0.01 kcal/mol/Å was achieved. The active sites of the proteins were defined based on the coordinates of the native co-crystallised ligands.

The three-dimensional structures of the ligands were obtained from the PubChem and/or Protein Data Bank databases and saved in Structure Data File (SDF) format. Ligands were protonated, partial charges were assigned, and energy minimisation was performed using the MMFF94 force field before docking. Docking simulations were carried out using the MOE Dock module, employing the Triangle Matcher placement method and the London dG scoring function for initial pose generation. The top 10 poses per ligand were retained and subsequently refined using the induced-fit protocol with rescoring by the Generalised Born Volume Integral / Weighted Surface Area (GBVI/WSA) dG function. Binding affinities were reported as docking scores (kcal/mol), and the most energetically favourable pose for each ligand–protein complex was selected for interaction analysis. The docked complexes were visualised and analysed using Discovery Studio Visualizer to identify hydrogen bonds, hydrophobic interactions, π–π stacking, and other key intermolecular contacts within the enzyme active sites.

To validate the reliability of the docking protocol, a redocking procedure was performed for each target protein. The native co-crystallised ligands associated with α-amylase (PDB ID: 1B2Y), α-glucosidase (PDB ID: 2QMJ), and XO (PDB ID: 3NVY) were extracted from their respective protein structures and re-docked into the corresponding active sites using the same docking parameters applied to the test ligands. The accuracy of the docking protocol was evaluated by calculating the root mean square deviation (RMSD) between the heavy atoms of the redocked ligand poses and their original crystallographic conformations. An RMSD value ≤ 2.0 Å was considered indicative of a valid and reliable docking protocol. The obtained RMSD values for all protein targets were within this acceptable threshold, confirming the suitability of the selected docking parameters, scoring functions, and active site definitions for subsequent ligand docking studies.

Statistical Analysis

All experiments were conducted in triplicate, and results were expressed as mean ± standard deviation (SD). Statistical analysis was performed using one-way analysis of variance (ANOVA) followed by Tukey's post hoc multiple comparison test. A significance level of $P < 0.05$ was considered statistically significant. GraphPad Prism, version 9.5.1 (GraphPad Software, San Diego, CA) was used for statistical analysis and IC_{50} determinations.

Ethics Approval

Ethical guidelines for in vitro and in silico studies were strictly adhered to. Ethical approval for the study was obtained from the POLAC Research Ethical Committee with reference number: PREC/2025/018.

RESULTS

Enzyme Inhibitory Activity of EAFOGL

The α-amylase and α-glucosidase inhibitory activities of the ethyl acetate fraction of *O. gratissimum* leaf extract (EAFOGL) were evaluated and compared with acarbose, a standard antidiabetic drug. EAFOGL demonstrated a concentration-dependent inhibition of both enzymes, with IC_{50} values of 87.17 ± 5.20 µg/mL for α-amylase and 49.84 ± 6.72 µg/mL for α-glucosidase (**Figure 1**). These values were higher than their respective acarbose values: 52.12 ± 2.74 and 40.94 ± 3.44 µg/mL, respectively, indicating moderate but promising inhibitory potential.

Antioxidant Activity of EAFOGL

EAFOGL exhibited significant antioxidant activity in both DPPH radical scavenging and metal chelation assays. The IC_{50} for DPPH scavenging was 90.32 ± 9.91 µg/mL, while metal chelation yielded an IC_{50} of 98.58 ± 13.29 µg/mL (**Figure 2**). These values, although higher than their respective standards, are ascorbic acid (59.07 ± 5.99 µg/mL) for DPPH and EDTA (70.11 ± 9.34 µg/mL) for metal chelation. These confirm the free radical-neutralising and pro-oxidant-suppressing potential of the fraction.

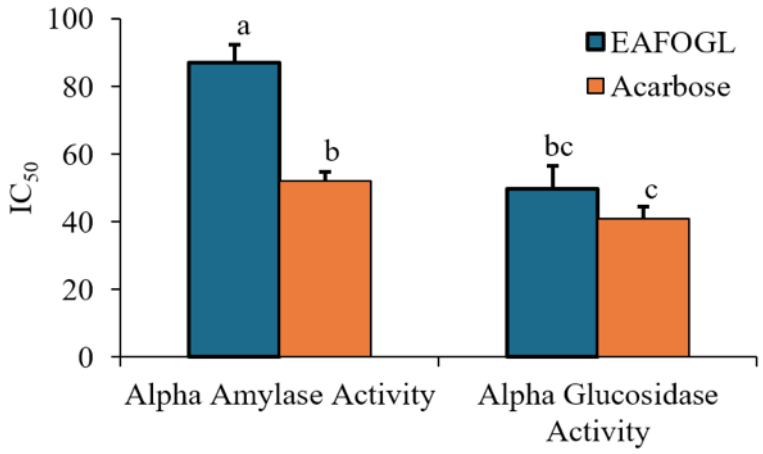

Figure 1: Inhibitory potentials of ethyl acetate fraction of *Ocimum gratissimum* leaves on α-amylase and α-glucosidase. NB: Bars with different letters are significantly different (α = 0.05); those with the same letter are not.

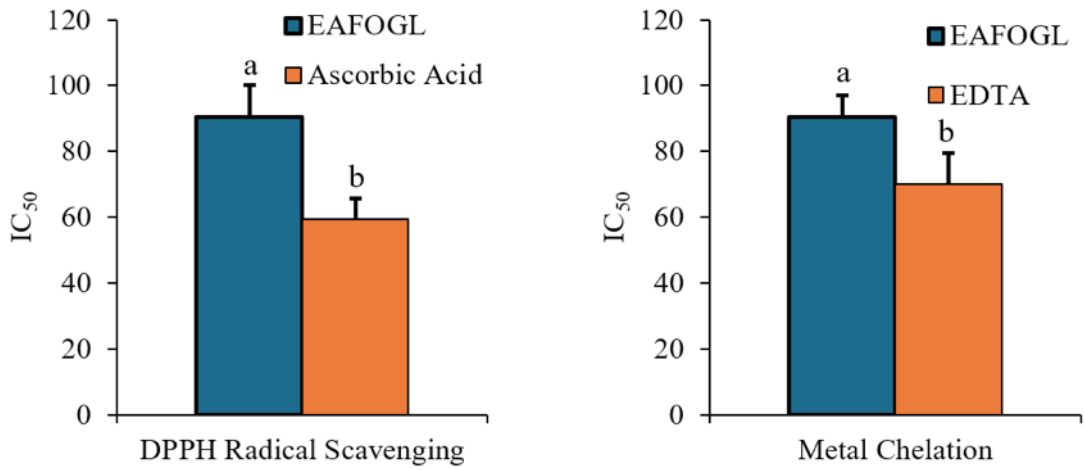

Figure 2: 2,2-Diphenyl-1-picrylhydrazyl radical scavenging and metal chelating potentials of ethyl acetate fraction of *Ocimum gratissimum* leaves. NB: Bars with different letters are significantly different (α = 0.05); those with the same letter are not.

Table 1: Result of LC-MS analysis of *Ocimum gratissimum* of Ethyl Acetate Fraction (OGEAF) showing *Mass-to-Charge Ratio* (MZ) (negative and positive modes), actual mass, and tentative compounds.

Retention Time (RT) (minutes)	Mode	m/z (MZ)	Neutral mass (Da)	Identified compound
1.980	−ESI	359.496	360.503	Trans-rosmarinic acid
2.605	+ESI	288.335	287.328	Eriodictyol
6.546	+ESI	237.684	236.677	Sesquiterpenoid
8.475	−ESI	359.155	360.162	Cis-rosmarinic acid
10.405	−ESI	343.893	344.900	Caffeoylshikimic acid

NB: Compounds obtained from https://massbank.eu/MassBank/Result.jsp, using MZ in −ESI $[M-H]^-$ and +ESI $[M+H]^+$ modes. Tolerance limit is ±5 ppm.

LC-MS Identification of Bioactive Compounds

LC-MS analysis revealed five tentative compounds in the EAFOGL: trans-rosmarinic acid, eriodictyol, sesquiterpenoid, cis-rosmarinic acid, and caffeoylshikimic acid, as depicted in **Table 1**. These compounds were tentatively identified based on their mass-to-charge (m/z) ratios and retention times using the MassBank database. The chemical structures of the respective identified compounds are depicted in **Figure 3**.

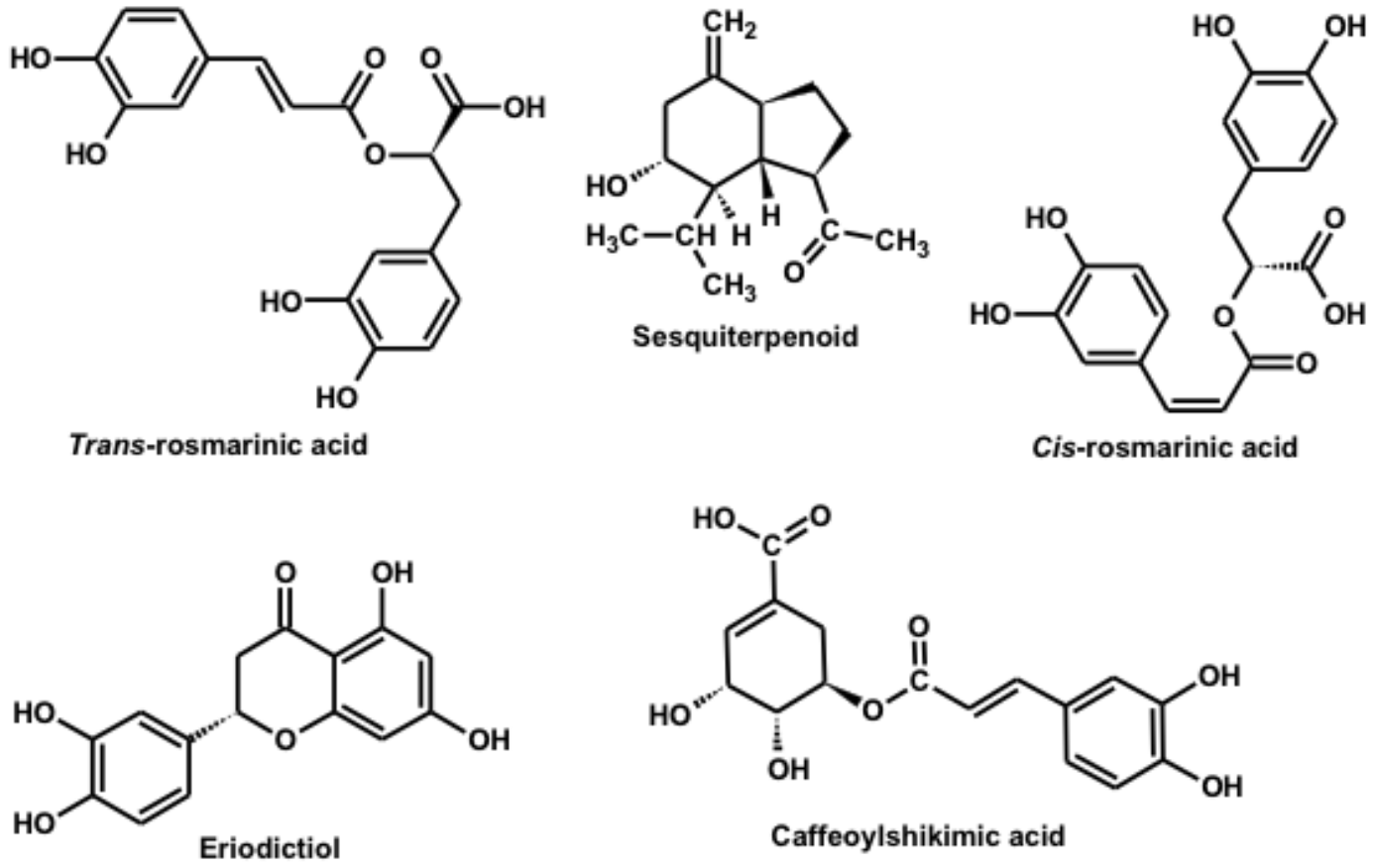

Figure 3: Chemical structures of the identified compounds through LC-MS analysis.

Molecular Docking Results

Molecular docking of selected phytochemicals against α-amylase (1B2Y), α-glucosidase (2QMJ), and XO (3NVY) is summarised in **Tables 2 to 4**. Docking protocol validation by re-docking the native ligands yielded RMSD values of 1.5393 Å, 1.8763 Å, and 1.3623 Å, respectively, confirming reliable reproduction of the crystallographic binding poses.

For α-amylase, the native ligand acarbose showed the strongest binding affinity (−10.5167 kcal/mol), forming multiple hydrogen bonds with key catalytic residues (Asp197, Glu233, Asp300) as presented in **Table 2**. Among the screened compounds, trans- and cis-rosmarinic acid exhibited the most favourable binding energies and interacted with essential active-site residues through hydrogen bonding and stabilising π-interactions, while caffeoylshikimic acid and eriodictyol showed moderate affinity. The sesquiterpenoid displayed comparatively weaker binding. **Figure 4** presents the top ligand–α-amylase (i.e., trans-rosmarinic acid-1B2Y_α-amylase) docking result, shown in (a) 3D and (b) 2D representations, generated using Discovery Studio Visualizer.

Against α-glucosidase, acarbose bound strongly (−8.8490 kcal/mol) via extensive interactions with catalytic residues (Asp203, Asp327, Asp443, Asp542, His600) as depicted in **Table 3**. Among the test ligands, caffeoylshikimic acid showed the highest affinity, followed by trans-rosmarinic acid and eriodictyol, whereas the sesquiterpenoid again exhibited the weakest interaction profile. **Figure 5** shows the top ligand–α-glucosidase docking result, depicted in (a) 3D and (b) 2D representations using Discovery Studio Visualizer.

In the XO system, the native ligand quercetin bound with an energy of −7.1842 kcal/mol. Notably, cis-rosmarinic acid demonstrated the strongest binding affinity among all screened compounds (−7.558 kcal/mol), exceeding that of quercetin, and formed extensive hydrogen bonding and π–π interactions with key residues (Phe914, Phe1009). Trans-rosmarinic acid and eriodictyol also showed binding affinities comparable to the native ligand, as depicted in **Table 4**. **Figure 6** presents the top ligand–XO docking result (Cis-Rosmarinic acid-3NVY), shown in (a) 3D and (b) 2D representations using Discovery Studio Visualizer.

Overall, rosmarinic acid isomers consistently exhibited favourable binding energies and key active-site interactions across all three enzymes, whereas the sesquiterpenoid showed limited affinity.

DISCUSSION

This study evaluated the antidiabetic and antioxidant potential of the ethyl acetate fraction of *O. gratissimum* leaves (EAFOGL) using in vitro enzyme inhibition and antioxidant assays, LC-MS phytochemical profiling, and in silico molecular

Table 2: Molecular docking results of selected ligands against α-amylase (PDB ID: 1B2Y), showing binding energies and key protein–ligand interactions.

Ligand	Docking score (kcal/mol)	H-bonds (No.)	Key interacting residues: α-amylase (PDB ID: 1B2Y)
Native ligand: Acarbose *RMSD (Å): 1.5393	–10.5167	11	HB: Thr163, His305, Asp300, Glu233, Gly306, Lys200,Tyr151, His201, Asp197, Gln63. CH: Gly306, Asp300. π+: Trp59. πA: His305
Caffeoylshikimic acid	–6.4434	6	HB: Gln63. His299, Asp197, Glu233. CH: His305. π–: Asp197. πLP: Trp59. ππS: Tyr62. πA: Trp59
Cis-Rosmarinic acid	–6.8046	4	HB: Asp197, Glu233, Tyr151, tyr62. ππS: Trp59. ππT: Trp58. πA: Ile235
Eriodictyol	–6.1120	5	HB: Asp197, His299, Glu233, Gln63. πLP: Trp59. ππS: Trp59, Trp62. ππT: 58.
Sesquiterpenoid	–5.6919	1	HB: Asp197. AA: Ala198, Leu162. πA: Tyr62
Trans-Rosmarinic acid	–6.8983	3	HB: Lys200, Asp197, His299. CH: Asp300. πσ: Ile235. πLP: Trp59. ππS: Trp59. ππT: His201. πA: Lys200

HB: conventional hydrogen bond; CH: carbon-hydrogen bond; π+: π-cation interaction; π–: pi-anion interaction; πA: pi-alkyl interaction; πLP: pi-lone pair; ππS: pi-pi stacked; ππT: pi-pi T-shaped; πσ: pi-sigma interaction; AA: alkyl-alkyl.

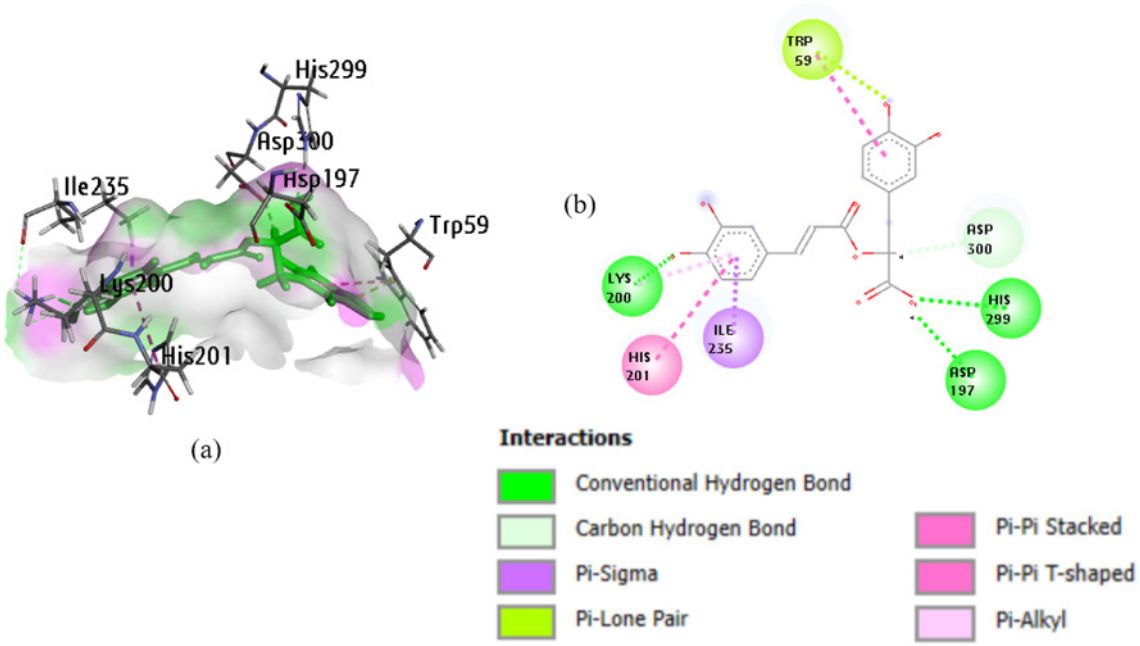

Figure 4: Best ligand–α-amylase docking pose (trans-rosmarinic acid_1B2Y) showing (a) 3D interaction within the enzyme active site and (b) 2D interaction map highlighting key hydrogen bonds and hydrophobic interactions, visualised using Discovery Studio Visualizer.

Table 3: Molecular docking results of identified compounds against α-glucosidase (PDB ID: 2QMJ).

Ligand	Docking score (kcal/mol)	H-bonds (No.)	Key interacting residues: α-glucosidase (PDB ID: 2QMJ)
Native ligand: Acarbose *RMSD (Å): 1.8763	–8.8490	8	AC: Asp203, Asp542, Asp443. HB: Met444, Asp443, Asp327, Asp542, Asp203, Arg202, His600. CH: Lys480, Asp327, Thr204, Asp443, Asp542. πA: Phe575.
Caffeoylshikimic acid	–6.5881	3	HB: His600, Asp443, Asp542. CH: Asp542, Asp443. π–: Asp203. πA: Tyr299, Phe575
Cis-Rosmarinic acid	–6.0048	7	HB: Asp203, Arg526, Asp443, Thr544. CH: Asp542. SX: Met444. ππT: Tyr299, Phe575. πA: Ala576.
Eriodictyol	–6.1120	3	HB: Asp327, Asp203. CH: Thr204. π–: Asp443, Asp542. ππS: Phe575, Tyr299.
Sesquiterpenoid	–4.6298	1	HB: Asp203. CH: Thr204, Asp542. AA: Ala576.
Trans-Rosmarinic acid	–6.1919	4	HB: Asp327, His600, Asp203. CH: Gln603, Asp542. π–: Asp443.

HB: conventional hydrogen bond; CH: carbon–hydrogen bond; π+: π-cation interaction; π–: pi-anion interaction; πA: pi-alkyl interaction; πLP: pi-lone pair; ππS: pi-pi stacked; ππT: pi-pi T-shaped; πσ: pi-sigma interaction, AA: alkyl-alkyl, AC: attractive charge, SX: sulphur-x interaction.

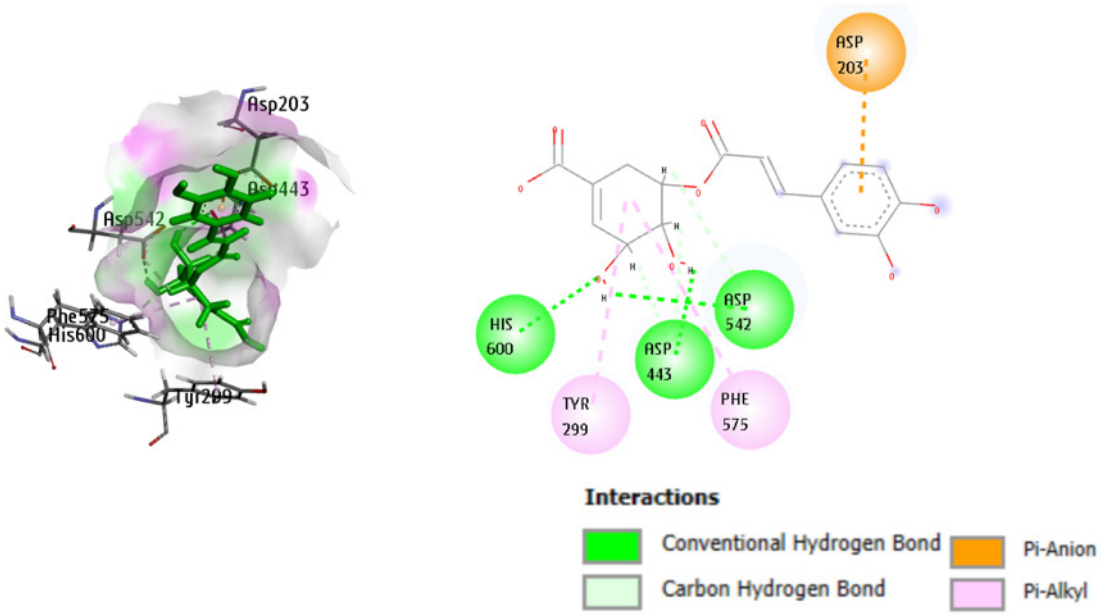

Figure 5: Best ligand-α-glucosidase docking pose (Caffeoylshikimic Acid-2QMJ) showing (a) 3D binding orientation within the catalytic pocket and (b) 2D interaction diagram illustrating key amino acid interactions, generated using Discovery Studio Visualizer.

Table 4: Molecular docking results of selected ligands against xanthine oxidase (PDB ID: 3NVY), showing binding energies and key protein-ligand interactions.

Ligand	Docking score (kcal/mol)	H-bonds (No.)	Key interacting residues: Xanthine Oxidase (PDB ID: 3NVY)
Native ligand: Quercetin *RMSD (Å): 1.3623	–7.1842	5	HB: Ala1079, Arg880, Thr1010, Val1011, Ser876. CH: Ala1079. πA: Phe575. ππS: Phe914. ππT: Phe1009. πA: Ala1078, Ala1079
Caffeoylshikimic acid	–6.7353	6	HB: Glu1261, glu802, thr1010, val1011, met770. CH: Ala1078, Lys771. πA: Pro1076, Leu1014. πS: Met770
Cis-Rosmarinic acid	–7.558	5	HB: Leu1014, Ser1075, Thr1010. CH: Lys771, Phe1009. ππS: Phe914. ππT: Phe1009, πA: Ala1079, Ala1078, Leu1014, Pro1076, Met770.
Eriodictyol	–6.9963	6	HB: Lys771, Glu802, Ala1079, Thr1010, Val1011. CH: Lys771. ππS: Phe914. ππT: Phe1009. πA: Leu1014, Leu648, Ala1078, Ala1079.
Sesquiterpenoid	–5.4008	3	HB: Thr1077, Glu802, Phe798. CH: Thr1077, Phe798. AA: Met770.
Trans-Rosmarinic acid	–7.0389	4	HB: Met770, Glu802, Ser876. πS: Met770. ππS: Phe914. ππT: Phe1009. πA: Lys771, Pro1076, Ala1078

HB: conventional hydrogen bond; CH: carbon–hydrogen bond; π+: π-cation interaction; π–: pi-anion interaction; πA: pi-alkyl interaction; πLP: pi-lone pair; ππS: pi-pi stacked; ππT: pi-pi T-shaped; πσ: pi-sigma interaction, AA: alkyl-alkyl; AC: attractive charge, SX: sulphur-x interaction; πS: pi-sulphur.

docking. EAFOGL demonstrated concentration-dependent inhibition of both α-amylase and α-glucosidase, two key enzymes involved in carbohydrate digestion and postprandial hyperglycaemia. Natural phenolic-rich extracts have been widely reported to inhibit these enzymes, supporting the use of phytochemicals in managing hyperglycaemia. [24–26]

Although EAFOGL exhibited higher IC_{50} values than acarbose, moderate inhibition, particularly of α-amylase, may be advantageous, as excessive α-amylase inhibition is associated with gastrointestinal side effects of synthetic inhibitors. Similar studies indicate that selective α-glucosidase inhibition and balanced enzyme suppression by plant extracts can effectively reduce postprandial glucose excursions while minimising adverse effects. [25] The comparatively stronger α-glucosidase inhibition observed for EAFOGL suggests potential efficacy in regulating glucose absorption at the intestinal brush border. [24] EAFOGL also exhibited significant antioxidant activity in DPPH radical scavenging and metal chelation assays. Phenolic compounds in plant extracts act as hydrogen donors and metal chelators, contributing to free radical neutralisation and mitigation of oxidative stress, a central factor in the development of diabetic complications. [25,27] Although the IC_{50} values obtained were higher than those of standard antioxidants, the results confirm the intrinsic radical-scavenging potential of EAFOGL.

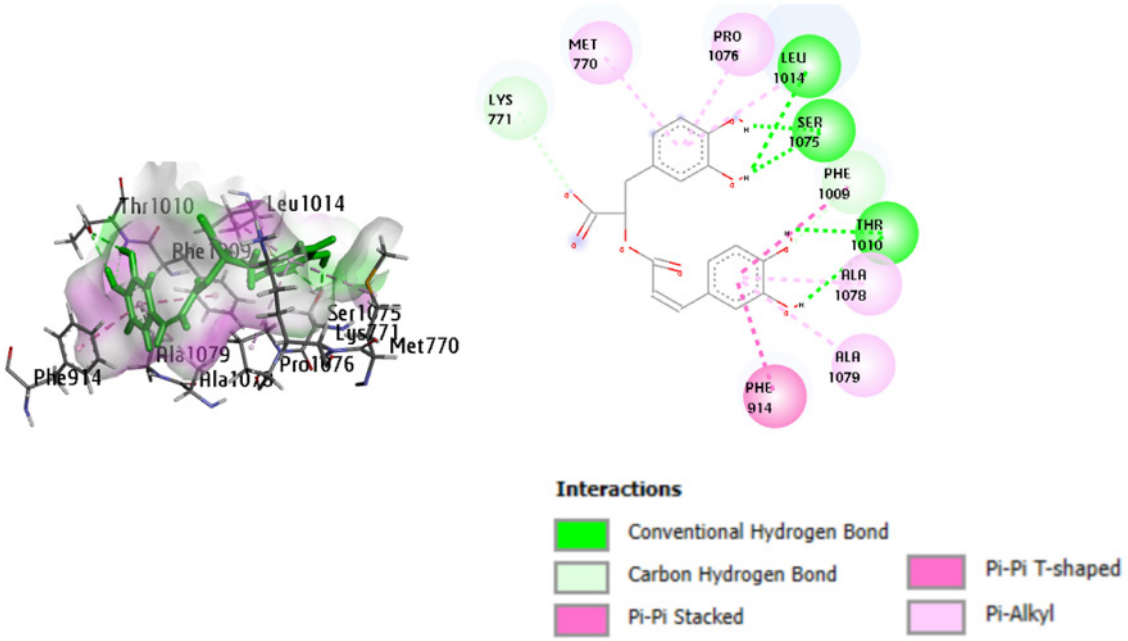

Figure 6: Best ligand-xanthine oxidase docking pose (Cis-Rosmarinic acid-3NVY) showing (a) 3D binding conformation at the active site and (b) 2D interaction profile indicating hydrogen bonding and hydrophobic contacts, visualised using Discovery Studio Visualizer.

LC-MS profiling tentatively identified phenolic and flavonoid compounds, including trans- and cis-rosmarinic acid, eriodictyol, and caffeoylshikimic acid, which have been documented in related species with antidiabetic and antioxidant activities. Rosmarinic acid, in particular, has been associated with both antioxidant and glucose-modulating effects and has been correlated with antidiabetic efficacy in aqueous extracts of *Ocimum* species. [28]

Molecular docking provided mechanistic support for the observed in vitro activities. Docking protocol validation produced RMSD values < 2.0 Å, confirming the reliability of the docking predictions. Against α-amylase, rosmarinic acid isomers exhibited favourable binding energies and interactions with catalytic residues such as Asp197 and Glu233, consistent with reports that polyphenolic compounds engage key enzyme active sites and inhibit catalytic function. [25,29] In the α-glucosidase system, caffeoylshikimic acid displayed the most favourable interactions among the test ligands, aligning with its relatively strong inhibitory profile. These docking patterns support the observed selective enzyme inhibition by EAFOGL. Docking against XO revealed that cis-rosmarinic acid exhibited a stronger binding affinity than the native ligand quercetin, interacting with aromatic residues critical to enzyme function. [30] Such interactions suggest that EAFOGL constituents may mitigate XO-mediated oxidative stress, consistent with the dual antioxidant and enzyme-inhibitory mechanisms of phenolic compounds reported in other plant studies. [24,31]

Overall, rosmarinic acid isomers consistently showed favourable binding across all targets, followed by caffeoylshikimic acid and eriodictyol. In contrast, the sesquiterpenoid exhibited weaker interactions, indicating less contribution to the bioactivity profile. The conjugated aromatic structures and multiple hydroxyl groups of the phenolic compounds likely facilitate hydrogen bonding, π–π, and electrostatic interactions with enzyme active sites.

Study Limitations

This study is limited by its reliance on in vitro assays, which may not fully reflect in vivo physiological conditions, including bioavailability, metabolism, and toxicity. Phytochemical identification was tentative, based on LC-MS data without further structural confirmation using spectroscopic techniques. Molecular docking provided predictive insights into enzyme–ligand interactions but did not account for protein dynamics or solvent effects, and enzyme kinetic analyses were not performed to elucidate inhibition mechanisms. Additionally, the use of a crude fraction rather than isolated compounds limits attribution of the observed bioactivities to specific phytochemicals.

CONCLUSIONS

In summary, this integrative in vitro and in silico evidence supports EAFOGL's dual antidiabetic and antioxidant potential, attributable to its phenolic constituents. These findings are congruent with existing literature on plant phenolics as nutraceutical agents capable of modulating carbohydrate-digesting enzymes and mitigating oxidative stress, and they justify further in vivo and pharmacokinetic studies to validate therapeutic applicability.

ACKNOWLEDGEMENTS

The authors of this article would like to express gratitude to Mallam Haruna Tsoho Bala from the Biochemistry Department at Bayero University Kano (BUK) for his support in laboratory investigative activities.

AUTHORS' CONTRIBUTION

Each author has made a substantial contribution to the present work in one or more areas, including conception, study design, conduct, data collection, analysis, and interpretation. All authors have given final approval of the version to be published, agreed on the journal to which the article has been submitted, and agree to be accountable for all aspects of the work.

SOURCE OF FUNDING

None.

CONFLICT OF INTEREST

None.

REFERENCES

1. International Diabetes Federation (IDF). Type 2 diabetes [Internet]. Brussels: IDF; 2025 [cited 2025 Nov 21]. Available from: https://idf.org/about-diabetes/types-of-diabetes/type-2/
2. World Health Organisation (WHO). Diabetes [Internet]. Geneva: WHO; 2024 [cited 2025 Nov 21]. Available from: https://www.who.int/en/news-room/fact-sheets/detail/diabetes
3. Clemente-Suárez VJ, Martín-Rodríguez A, Beltrán-Velasco AI, Rubio-Zarapuz A, Martínez-Guardado I, Valcárcel-Martín R, et al. Functional and therapeutic roles of plant-derived antioxidants in type 2 diabetes mellitus: Mechanisms, challenges, and considerations for special populations. Antioxidants (Basel). 2025;14(6):725.
4. Kasai S, Kokubu D, Mizukami H, Itoh K. Mitochondrial reactive oxygen species, insulin resistance, and Nrf2-mediated oxidative stress response-toward an actionable strategy for anti-aging. Biomolecules. 2023;13(10):1544.
5. Shirkhan F, Mirdamadi S, Mirzaei M, Akbari Adergani B, Nasoohi N. In-vitro investigation of antidiabetic and antioxidants properties of major prebiotics and plant based dietary fibers. J Diabetes Metab Disord. 2025; 24(1):105.
6. Ogunyemi OM, Adeyeye EO, Macaulay OS, Olabuntu BA, Achem J, Gyebi GA, et al. Machine learning-based QSAR and molecular modeling identify promising PTP1B modulators from Ocimum gratissimum for type 2 diabetes therapy. Mol Divers. 2025;29:387–403. doi:10.1007/s11030-025-11255-x.
7. Bose N, Pal TK. Variation of antioxidant properties of African basil (*Ocimum gratissimum*) leaves with respect to various drying and solvents extraction methods. Int J Front Life Sci Res. 2025;8(1):20-29.
8. Okoduwa SIR, Umar IA, James DB, Inuwa HM. Anti-diabetic potential of *Ocimum gratissimum* leaf fractions in fortified diet-fed streptozotocin treated rat model of type-2 diabetes. Medicines (Basel). 2017;4(4):73.
9. Shittu ST, Oyeyemi WA, Lasisi TJ, Shittu SA, Lawal TT, Olujobi ST. Aqueous leaf extract of *Ocimum gratissimum* improves hematological parameters in alloxan-induced diabetic rats via its antioxidant properties. Int J Appl Basic Med Res. 2016;6(2):96-100.
10. Ali H, Houghton PJ, Soumyanath A. alpha-Amylase inhibitory activity of some Malaysian plants used to treat diabetes; with particular reference to *Phyllanthus amarus*. J Ethnopharmacol. 2006;107(3):449-455.
11. Mohanraj K, Karthikeyan BS, Vivek-Ananth RP, Chand RP, Aparna SR, Mangalapandi P, et al. IMPPAT: A curated database of Indian medicinal plants, phytochemistry and therapeutics. Sci Rep. 2018;8(1):4329.
12. Bravard A, Bonnard C, Durand A, Chauvin MA, Favier R, Vidal H, et al. Inhibition of xanthine oxidase reduces hyperglycemia-induced oxidative stress and improves mitochondrial alterations in skeletal muscle of diabetic mice. Am J Physiol Endocrinol Metab. 2011;300(3):E581-E591.
13. Pasupuleti VR, Arigela CS, Gan SH, Salam SKN, Krishnan KT, Rahman NA, et al. A review on oxidative stress, diabetic complications, and the roles of honey polyphenols. Oxid Med Cell Longev. 2020;2020:8878172.
14. Liu N, Xu H, Sun Q, Yu X, Chen W, Wei H, et al. The role of oxidative stress in hyperuricemia and xanthine oxidoreductase (XOR) inhibitors. Oxid Med Cell Longev. 2021;2021:1470380.
15. Dev-Sharma A, Kaur I, Angish S, Thakur A, Sania S, Singh A. Comparative phytochemistry, antioxidant, antidiabetic, and anti-inflammatory activities of traditionally used *Ocimum basilicum* L. *Ocimum gratissimum* L., and *Ocimum tenuiflorum* L. BioTechnologia (Pozn). 2022; 103(2):131-142.
16. Motulsky H, Christopoulos A. Fitting Models to Biological Data Using Linear and Nonlinear Regression: A Practical Guide to Curve Fitting. Oxford: Oxford University Press; 2004.
17. Lawal TA. Screening of aqueous extract of *Persea americana* seeds for alpha-glucosidase inhibitors. Biochem Res Int. 2022;2022:3492203.
18. Gulcin İ, Alwasel SH. DPPH radical scavenging assay. Processes. 2023;11(8):2248.
19. Gulcin İ, Alwasel SH. Metal ions, metal chelators and metal chelating assay as antioxidant method. Processes. 2022;10(1):132.
20. Pang B, Zhu Y, Lu L, Gu F, Chen H. The applications and features of liquid chromatography-mass spectrometry in the analysis of traditional Chinese medicine. Evid Based Complement Alternat Med. 2016;2016:3837270.
21. Abilkassymova A, Aldana-Mejía JA, Katragunta K, Kozykeyeva R, Omarbekova A, Avula B, et al. Phytochemical screening using LC-MS to study antioxidant and toxicity potential of methanolic extracts of *Atraphaxis pyrifolia* Bunge. Molecules. 2024;29(18):4478.
22. Breaud C, Lallemand L, Mares G, Mabrouki F, Bertolotti M, Simmler C, et al. LC-MS based phytochemical profiling towards the identification of antioxidant markers in some endemic *Aloe* species from Mascarene islands. Antioxidants (Basel). 2022;12(1):50.
23. Lawal TA, Sholadoye QO, Ononamadu CJ, Musa B, Akinjoko VO, Segba DE. Evaluation of antioxidant and antidiabetic properties of ethyl acetate fraction from *Anacardium occidentale* leaves, in-vitro and in-silico. Acta Pharma Rep. 2024;3(2):23-40.
24. Febriyanti RM, Indradi RB, Maisyarah IT, Iskandar Y, Susanti RD, Lestari D. Alpha-amylase and alpha-glucosidase enzymes inhibition and antioxidant potential of selected medicinal plants used as anti-diabetes by Sundanese community in West Java, Indonesia. BMC Complement Med Ther. 2025;25(1):426.
25. Swargiary A, Roy MK, Mahmud S. Phenolic compounds as α-glucosidase inhibitors: A docking and molecular

dynamics simulation study. J Biomol Struct Dyn. 2023; 41(9):3862-3871.
26. Paun G, Neagu E, Albu C, Savin S, Radu GL. In vitro evaluation of antidiabetic and anti-inflammatory activities of polyphenolic-rich extracts from *Anchusa officinalis* and *Melilotus officinalis*. ACS Omega. 2020; 5(22):13014-13022.
27. Güven L, Erturk A, Miloğlu FD, Alwasel S, Gulcin İ. Screening of antiglaucoma, antidiabetic, anti-Alzheimer, and antioxidant activities of *Astragalus alopecurus* pall-analysis of phenolics profiles by LC-MS/MS. Pharmaceuticals (Basel). 2023;16(5):659.
28. Berhow MA, Affum AO, Gyan BA. Rosmarinic acid content in antidiabetic aqueous extract of *Ocimum canum* Sims grown in Ghana. J Med Food. 2012;15(7): 611-620.
29. Rasouli H, Hosseini-Ghazvini SM, Adibi H, Khodarahmi R. Differential α-amylase/α-glucosidase inhibitory activities of plant-derived phenolic compounds: A virtual screening perspective for the treatment of obesity and diabetes. Food Funct. 2017;8(5):1942-1954.
30. Etsassala NGER, Badmus JA, Marnewick JL, Iwuoha EI, Nchu F, Hussein AA. Alpha-glucosidase and alpha-amylase inhibitory activities, molecular docking, and antioxidant capacities of *Salvia aurita* constituents. Antioxidants (Basel). 2020;9(11):1149.
31. Görmez G, Yüksek V, Usta A, Dede S, Gümüş S. Phenolic contents, antioxidant activities, LCMS profiles of *Mespilus germanica* leaf extract and effects on mRNA transcription levels of apoptotic, autophagic, and necrotic genes in MCF7 and A549 cancer cell lines. Cell Biochem Biophys. 2024;82(3):2141-2155.